MDPI

Article

Platinum-Group Minerals in the Placer of the Kitoy River, East Sayan, Russia

Evgenia V. Airiyants *, Olga N. Kiseleva, Sergey M. Zhmodik, Dmitriy K. Belyanin [ID] **and Yuriy C. Ochirov**

Sobolev Institute of Geology and Mineralogy, Siberian Branch of the Russian Academy of Sciences, 630090 Novosibirsk, Russia; kiseleva_on@igm.nsc.ru (O.N.K.); zhmodik@igm.nsc.ru (S.M.Z.); bel@igm.nsc.ru (D.K.B.); ochirovjuri@mail.ru (Y.C.O.)

* Correspondence: jenny@igm.nsc.ru; Tel.: +7-983-303-38-61

Abstract: The platinum-group minerals (PGM) in placer deposits provide important information on the types of their primary source rocks and ores and formation and alteration conditions. The article shows for the first time the results of a study of placer platinum mineralization found in the upper reaches of the Kitoy River (the southeastern part of the Eastern Sayan (SEPES)). Using modern methods of analysis (scanning electron microscopy), the authors studied the microtextural features of platinum-group minerals (PGM), their composition, texture, morphology and composition of microinclusions, rims, and other types of changes. The PGM are Os-Ir-Ru alloys with a pronounced ruthenium trend. Many of the Os-Ir-Ru grains have porous, fractured, or altered rims that contain secondary PGE sulfides, arsenides, sulfarsenides, Ir-Ni-Fe alloys, and rarer selenides, arsenoselenides, and tellurides of the PGE. The data obtained made it possible to identify the root sources of PGM in the placer and to make assumptions about the stages of transformation of primary igneous Os-Ir-Ru alloys from bedrock to placer. We assume that there are several stages of alteration of high-temperature Os-Ir-Ru alloys. The late magmatic stage is associated with the effect of fluid-saturated residual melt enriched with S, As. The post-magmatic hydrothermal stage (under conditions of changing reducing conditions to oxidative ones) is associated with the formation of telluro-selenides and oxide phases of PGE. The preservation of poorly rounded and unrounded PGM grains in the placer suggests a short transport from their primary source. The source of the platinum-group minerals from the Kitoy River placer is the rocks of the Southern ophiolite branch of SEPES and, in particular, the southern plate of the Ospa-Kitoy ophiolite complex, and primarily chromitites.

Keywords: platinum-group minerals; placer deposits; ophiolite complexes; East Sayan; Russia

1. Introduction

Chromitites and platinum-group elements (PGE) mineralization in ophiolite complexes have been studied by many researchers worldwide [1–14]. Chromitites from ophiolite complexes, particularly Cr-rich varieties, commonly contain PGE mineralization with predominant Os, Ir, and Ru [15]. These elements are assigned to refractory PGE of the Ir subgroup (IPGE = Os, Ir, Ru), in contrast to low-melting PGE (Pd subgroup (PPGE = Rh, Pt, Pd)) [2]. Minerals of IPGE are usually associated with Cr-rich chrome-spinel, forming intergrowths or inclusions to yield mantle parageneses [16]. On the other hand, recent studies of PGE remobilization indicate that refractory PGE are mobile in the case of chromitite alteration [17–19].

The podiform chromitites and PGE mineralization of the ultrabasic massifs and ophiolite complexes within the Central Asian fold belt (Altai-Sayan region) have been investigated in some previous studies, including the ultrabasic massifs in ophiolite complexes of Tuva [20], Western Sayan (Kalna ultrabasic massif [21], Aktovrakskiy complex [22–24]), and Eastern Sayan (Ospa-Kitoy ultrabasic massif [25–29]). However, there are only a few records of PGE mineralization in alluvial sediments in the Eastern Sayan [30], and there are practically no detailed studies. In this article, for the first time, PGM from the Kitoy River

placer are described and studied in detail. The purposes of our research are the following: to characterize the PGE mineralogy of the placer; to examine mineral associations, compositional ranges, and extents of solid solutions; to examine types of various micrometric inclusions hosted by placer grains of PGE alloy minerals and types of alteration rims; and to suggest a potential lode source for the placer occurrences of PGM of the Kitoy River placers, on the basis of the results obtained and data from previous studies.

2. Geological Setting

The study area is the southeastern part of the Eastern Sayan (SEPES)—a territory formed mainly during the Neoproterozoic-Early Paleozoic. In this area, there is a multistage tectonics and tectonomagmatic processing of autochthonous and thrust allochthonous oceanic (ophiolite), island-arc, and marginal-marine terranes, as well as amalgamation of accretion-collisional and post-collisional magmatic complexes that arose during opening and subsequent closing of the margins structures of the Paleo-Asian ocean [31–33]. In generalized form, the geological structure of the region is determined by the presence of the Gargan paleocontinent of the Meso- to Neoarchean age, with a carbonate cover of the Meso- to Neoproterozoic age. Sublatitudinal branches (belts) of ophiolite associations encircle the Gargan paleocontinent from the north and south.

Previous researchers have obtained data on the complex structure and heterogeneity of these ophiolite branches [27,28,31,34,35]. The Dunzhugur, Khara-Nur, Halbyn-Khairkhan and the northern plate of the Ospa-Kitoi "massif" represents the Northern (Dunzhugur) ophiolite branch. The ophiolites of the Northern branch were formed in the setting of island arcs. Restite dunites and harzburgites, rocks of the transitional complex—wehrlite, pyroxenite, gabbro, complex of dikes of the boninite and calc-alkaline series and basaltic pillow lavas, with the flysch-type sedimentary sequences overlying the upper part by the ophiolite massif [34,36,37]. Chromite ore occurrences are localized in talc-carbonate rocks with quartz veins developed in the zone of intense changes in serpentinites [29].

The Southern (Ilchirsky) branch is represented by an almost continuous chain of ophiolite "massifs": the southern plate of the Ospa-Kitoy "massif", the Samarta and Ilchir complexes (cover fragments). Ophiolite complexes of the Southern branch were formed in the setting of mid-oceanic ridges [28,29,31,34,37–39]. In recent years, researchers have also identified the Middle ophiolite branch (Ulan-Sar'dag massif) [33,40]. The Middle and Southern branches are composed of tectonic nappes and clippes of oceanic ultramafic-mafic rocks, cumulative and layered gabbros, interbedded with plates of the Ilchir and Bokson allochthonous complexes, which contain sheets of olistostrome and melange, obducted onto the carbonate cover of the Gargan microcontinent [33]. In the composition of ophiolites, the most common mantle peridotites are dunites, harzburgites; wehrlite and pyroxenite are less common. Metavolcanic rocks of the alkaline type are located in the contact zone with serpentinites melange and are represented by rocks of the island-arc association—boninites, basalts, andesites, dacites. Podiform chromitites in them form schlieren, lenticular, and veinlet bodies with which the development of PGE mineralization is associated [41,42].

The Kitoy River is one of the largest and longest rivers in the Eastern Sayan. It originates from the confluence of the Ulzyta and Samarta rivers and flows from west to east through the entire SEPES territory. The valley of the Kitoy River (in the upper reaches) cuts through siliceous-carbonate deposits of the Boxonskaya series (V-O), volcanogenic-sedimentary deposits of the Barungolskaya formation (O-S), and terrigenous deposits of the Sagansayrskaya formation (D-C$_1$) (Figure 1). These sediments form the tectonic covers of the Ilchir structural-formation zone, overlapping the ophiolites of the Southern branch. The rocks of the ophiolite complex are exposed in the upper reaches of the Kitoy River and drained by its northern tributaries. In the alluvial sediments of the Kitoy River near the confluence of the Sagan-Sayr River, in the process of geological exploration, platinum-group minerals (PGM) were identified among the minerals of the heavy fraction.
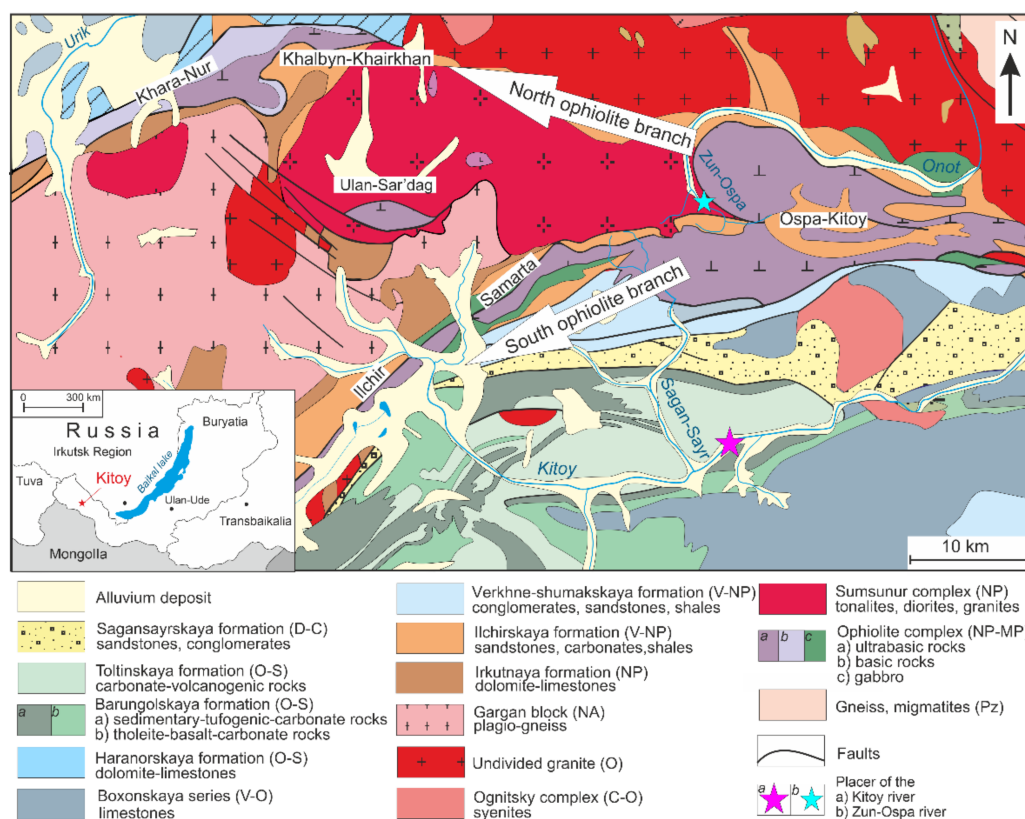
Figure 1. Geological map of the southeastern part of the Eastern Sayan region [32].

In this paper, we first describe the occurrences and mineralogical characteristics of assemblages of PGM in the alluvial placer associated with the River Kitoy. The results of our study allow us to draw conclusions about the sources of platinum-metal mineralization in the alluvial deposits of the Kitoy River, the stages and conditions of mineral formation of PGE mineralization. The PGM in placer deposits provide important information about the types of their primary source rocks and ores, as well as about the conditions of their formation and change.

3. Materials and Methods

3.1. Materials

This study presents the compositions of 30 grains of PGM, obtained from a private mineralogical collection of geologist Yu. Ch. Ochirov. During the period of geological exploration for placer gold with the sample selection of alluvial deposits of the Kitoy River 2–3 km below the confluence of the left tributary of the Sagan-Sayr River, he found grains of PGM among the heavy fraction minerals. The heavy minerals concentrated from alluvial sediments in the Kitoy River were obtained using the sluicing method, where water-sediment slurry is directed through multiple sluice boxes lined with riffles that segregate the heavy minerals, including gold and PGM, from the light fragments of bedrock. The grains we have studied were hand-picked from the sluice concentrate due to their interesting color, shape, or distinct appearance. Therefore, it is possible that the collection is biased and primarily contains grains of a certain composition. For this reason, we are not attempting to interpret the productivity or relative contribution of potential PGM sources.

The concentrates are composed of grains of chromian spinel (~50–75 vol.%), magnetite (up to ~30%), amphibole (up to ~10%), a small amount (<5%) of olivine, chlorite, and serpentine, and single grains of PGM. We examined 30 PGM grains found in heavy-mineral concentrates collected from alluvial deposits of the Kitoy River. We found that all detrital PGM grains represent Os-Ir-Ru alloys. The grain size does not exceed 1 mm across. They usually have a slightly rounded shape; idiomorphic grains with a well-preserved hexagonal

shape and crystal clusters are less common (Figure 2). Many placer grains of Os-Ir-Ru alloys have a fractured or altered rim associated with the development of secondary phases of PGE sulfide, arsenide, and sulfarsenide. Rare compounds are present also in these rims—tellurides and Se-rich arsenides of PGE. In individual cases, secondary changes almost completely replace the original grain. The grains rarely contain microinclusions. In some grains, we recorded inclusions of both platinum-group minerals and silicate minerals (biotite, amphibole, serpentine) and base-metal sulfides.
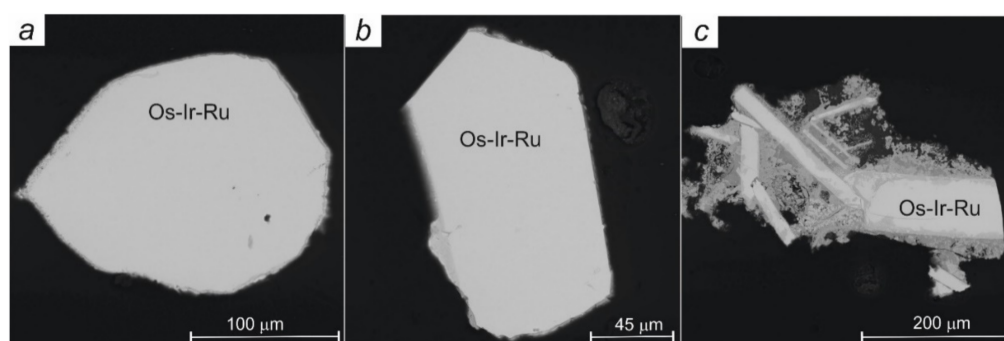

Figure 2. Back-scattered electron (BSE) images showing morphological and textural features of placer grains PGM from the alluvial placer of the r. Kitoy: (**a**) a partly round grain Os-Ir-Ru alloy; (**b**) hexagonal idiomorphic grain Os-Ir-Ru alloy; (**c**) intergrowths of subidiomorphic crystals of Os-Ir-Ru alloy.

3.2. Analytical Methods

The chemical composition and morphology of PGMs was determined using a MIRA 3 LMU scanning electron microscope, with an attached INCA Energy 450 XMax 80 microanalysis energy dispersive system, at the Sobolev Institute of Geology and Mineralogy, Russian Academy of Science (Analytical Center for multi-elemental and isotope research SB RAS). We employed an accelerating voltage of 20 kV, a beam current of 1600 pA, an energy resolution (MIRA) of 126–127 eV at the Mn Kα line, and a region (3–5 μm), depending on the average atomic number of the sample and the wavelength of analytical line. The live time of spectrum acquisition was 30 seconds; in some cases, it reached 150 seconds. The standards used were FeS_2 (S), $FeAs_2$ (As), HgTe (Hg), PbTe (Pb and Te), and pure metals (Fe, Co, Ni, Cu, Ru, Rh, Pd, Ag, Sb, Os, Ir, Pt, and Au). The minimum detection limits of the elements (wt. %) were found to be 0.1–0.2 for S, Fe, Co, Ni, and Cu; 0.2–0.4 for As, Ru, Rh, Pd, Sb, and Te; and 0.4–0.7 for Os, Ir, and Pt. The analytical error for the main components does not exceed 1–2 rel. %.

4. Results

4.1. Grains of Os-Ir-Ru Alloys

As noted, all studied detrital PGM grains consist of an Os-Ir-Ru alloy. We did not observe any zoning in the grains. There are minor variations in the chemical composition associated with the appearance of alloys more enriched with ruthenium or osmium (Table 1). The PGM of the Kitoy River placer occupy a narrow field of solid solution in the system (Figure 3) with a pronounced ruthenium trend. The observed Ru-enrichment points to the accumulation of levels of Ru during crystallization. Insignificant impurities of Fe, less commonly Ni, in the chemical composition of the alloys were noted. Of special interest is the presence in almost all grains of Rh from 0.2 g/t to 2.5 g/t, as well as Pt, which occurs in 50% of alloys and reaches 4 g/t. There is a direct correlation between the concentrations of Pt and Rh in alloys—we noted the highest content of rhodium in grains with an impurity of platinum. Sufficiently high platinum contents in the initial melt led to the appearance of idiomorphic Pt-Fe alloy inclusions in the matrix during cooling of the system, corresponding in stoichiometric composition to isoferroplatinum (Figure 4). It

appears that Pt behaved somewhat incompatibly during the crystallization of the Os-Ir-Ru alloy [16,43–46].

Table 1. Compositions of grains of Ru-Os-Ir alloy from the Placer of the Kitoy River (wt.%).

No.		Ru	Os	Ir	Rh	Pt	Fe	Ni	Cu	Total
1	Ru-dominant	25.74	39.16	28.08	0.85	3.38	0.33	bdl	bdl	97.21
2		25.58	38.7	32.9	0.91	bdl	0.14	bdl	bdl	98.09
3		30.96	34.35	29.45	0.82	2.56	0.23	bdl	bdl	98.14
4		30.93	34.94	28.22	1.13	3.96	0.3	0.28	bdl	99.18
5		29.34	36.88	29.51	bdl	bdl	0.43	bdl	bdl	95.73
6		26.77	39.19	26.83	2.55	4.02	0.33	bdl	bdl	99.36
7	Os-dominant	10.31	50.62	36.3	0.65	bdl	0.41	bdl	bdl	97.88
8		11.26	49.87	37.05	0.22	bdl	0.05	bdl	bdl	98.4
9		23.17	51.21	20.68	0.8	1.55	0.2	bdl	bdl	97.41
10	matrix	14.95	47.31	36.46	0.59	bdl	0.48	bdl	bdl	99.79
	Inclusion	bdl	bdl	bdl	2.18	81.35	10.03	1.61	2.2	97.37
11	Os-Ir-Ru	18.86	43.83	34.55	0.12	bdl	0.36	0.37	bdl	97.36
12		16.76	44.47	34.22	bdl	1.79	0.29	bdl	bdl	97.24
13		15.63	44.45	34.38	0.28	1.6	0.275	0.4	bdl	96.34
14	matrix	21.27	40.3	34.69	1.52	1.23	0.43	0.44	bdl	99.01
	Inclusion	bdl	bdl	bdl	1.18	82.4	10.29	1.38	2.42	97.67
Atomic proportions (per a total of 100 at%)										
		Ru	Os	Ir	Rh	Pt	Fe	Ni	Cu	Total
1	Ru-dominant	39.9	32.27	22.89	1.3	2.72	0.92	0		100
2		39.61	31.85	26.77	1.38	0	0.39	0		100
3		46.03	27.14	23.06	1.19	1.97	0.61	0		100
4		45.14	27.1	21.66	1.62	2.99	0.79	0.7		100
5		44.61	30.62	23.59	0	0	1.18	0		100
6		39.94	31.25	21.05	3.73	3.04	0.99	0		100
7	Os-dominant	17.86	46.64	33.1	1.11	0	1.29	0		100
8		19.61	45.75	33.97	0.67	0	0	0		100
9		37.15	43.76	16.77	1.41	0.63	0.28	0		100
10	matrix	17.86	46.64	33.1	1.11	0	1.29	0		100
	Inclusion				3.11	61.33	26.43	4.03	5.09	100
11	Os-Ir-Ru	30.81	37.18	29.69	0.19	0	1.08	1.05		100
12		28.01	39.49	30.07	0	1.55	0.88	0		100
13		26.21	39.64	30.32	0.46	1.39	0.83	1.15		100
14	matrix	33.26	32.41	28.52	2.33	1.1	1.22	1.16		100
	Inclusion				1.69	62.14	27.12	3.46	5.60	100

Note. Results of EDS analysis are listed in weight%; "bdl" indicates that amounts of elements are below detection limits.
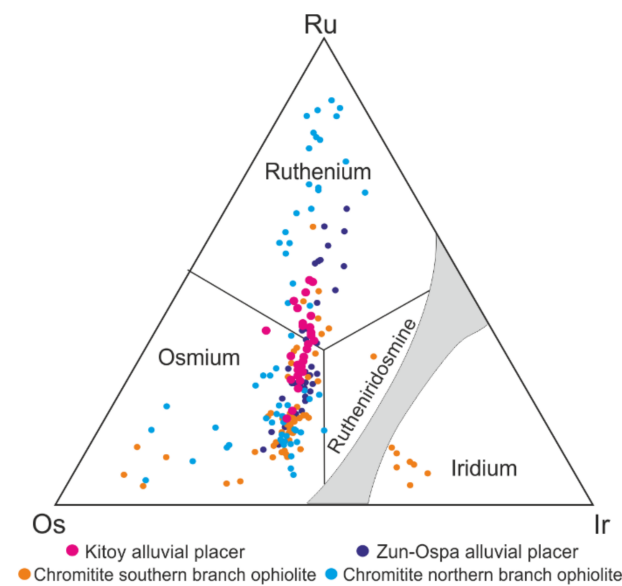
Figure 3. Compositional variations of grains of Os-Ir-Ru alloys from the Kitoy placer (this study), in comparison with Os-Ir-Ru alloys from the Zun-Ospa deposit, East Sayan [30], Os-Ir-Ru alloys from chromitites South and North ophiolite branches [28,29] in terms of the Os-Ir-Ru diagram (at.%). The miscibility gap and nomenclature are based on [47].
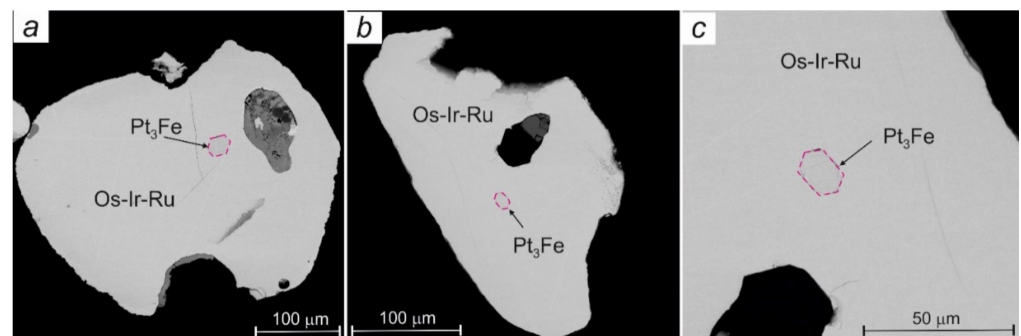

Figure 4. BSE images showing idiomorphic inclusions of Pt-Fe alloy hosted by a grain of Os-Ir-Ru alloy: (**a**) A partly rounded grain of Os-Ir-Ru alloy containing an idiomorphic inclusion of Pt-Fe-alloy; (**b**) silicate inclusion and inclusion of isoferroplatinum in Os-Ir-Ru alloy; (**c**) idiomorphic inclusion of isoferroplatinum in Os-Ir-Ru alloy.

For comparison, we plotted on the ternary diagram the compositions of the Os-Ir-Ru alloys studied by us from the chromitites of the ophiolite complexes of SEPES [28,29,39,41,42]. With general regularities in the distribution of Os-Ir-Ru in PGM grains, there are some differences in the composition of PGMs from chromitites of the southern and northern ophiolite branches of SEPES. The Os-Ir-Ru alloy grains from the chromitites of the southern ophiolite branch and, in particular, the southern plate of the Ospa-Kitoy ophiolite complex, have higher iridium contents. In the chromitites of the northern ophiolite branch, we observed alloys most enriched in ruthenium. In the alluvial placers of the Zun-Ospa River draining the northern part of the Ospa-Kitoy ophiolites complex (northern ophiolite branch), the Os-Ir-Ru alloy also reached higher ruthenium values [30].

The observed micro-textural features of the grains reflect the terms and conditions of crystallization of the PGM. The earliest, primary mineral among the studied PGMs are grains having a massive, homogeneous microtexture, in some cases with rare aluminum-silicate inclusions formed as a result of the capture of the primary melt. In addition, some of the studied PGM grains have superimposed textures formed during hydrothermal-metasomatic changes. They are represented by micro-zonal, micro-striped, micro-breccia

textures (Figure 5). Among the minerals forming these textures, sulfides, arsenides and sulfo-arsenides of PGE, and selenotelluride compounds of PGE were established.
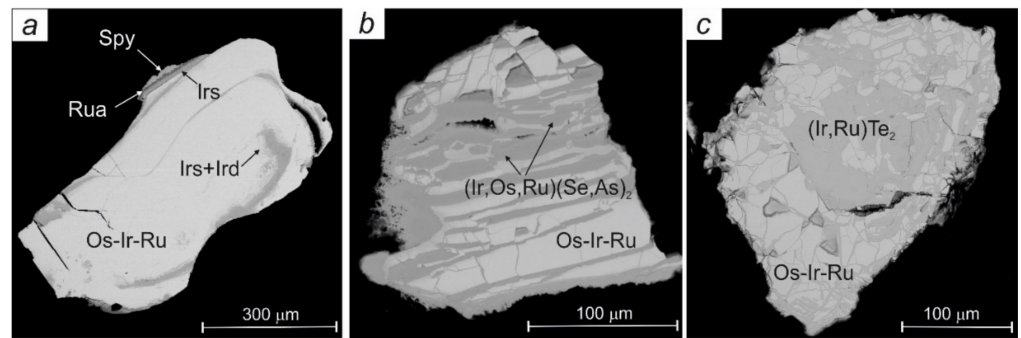

Figure 5. BSE images showing secondary textures metasomatic alteration of Os-Ir-Ru alloys: (**a**) micro-zonal texture with zones composed of sulfoarsenides (irarsite (Irs), ruarsite (Rua)) and arsenides (iridarsenite (Ird), sperrylite (Spy), (**b**) micro-striped texture with zones formed by arsenoselenides, (**c**) micro-breccia texture in a deformed primary Os-Ir-Ru grain are cemented by tellurides of the PGE.

4.2. Inclusions in Grains of Os-Ir-Ru Alloys

Inclusions in our PGM grains are rare. We identified several types among them. The first type is interpreted as melt or melt + fluid inclusions captured during crystallization; these appear as silicate inclusions altered to varying degrees. Most commonly, they are composed of a calcic amphibole, namely magnesio-hornblende. We also identified magnesian olivine (Fo-90), biotite, and chlorite in the inclusions (Figure 6a–c). We present data on the chemical composition of silicate inclusions in Table 2 and for comparison give the compositions of silicate inclusions in chromian spinel and PGMs from various ultrabasic-basic complexes [46,48,49].
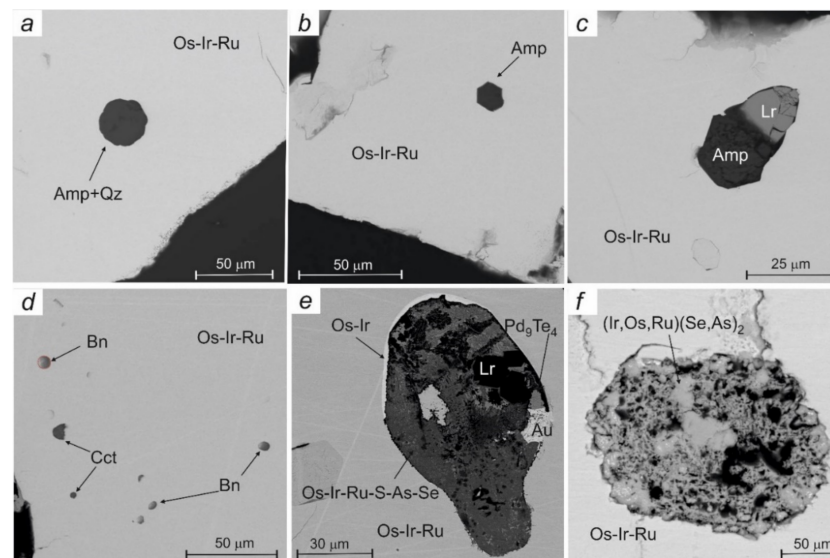
Figure 6. BSE images showing of inclusion in Os-Ir-Ru alloys: (**a**) drop-shaped inclusion interpreted to represent a silicate melt; (**b**) inclusion of magnesio-hornblende (Amp); (**c**) two-phase inclusion of magnesio-hornblende (Amp) and laurite (Lr); (**d**) base-metal sulfide inclusions: bornite (Bn) and chalcocite (Cct); (**e**) polyphase inclusion with idiomorphic laurite (Lr) and telluropalladinite in intergrowth with gold (Au) in a mixture of arsenoselenides and sulfides IPGE with a thin border of Os-Ir composition; (**f**) inclusion filled with arsenoselenides of the IPGE.

Table 2. Chemical composition of the silicate inclusions in the PGM of the Kitoy River according to the EDS data (wt.%) compared to the silicate inclusions in the chromian spinel from different ultrabasic-basic complexes (wt.%).

	Mineral	SiO$_2$	TiO$_2$	Al$_2$O$_3$	Cr$_2$O$_3$	FeO	MnO	MgO	NiO	CaO	Na$_2$O	K$_2$O	Total	Matrix
The authors' data	olivine	40.63				5.85		52.16	0.47				99.11	
	olivine	41.61				5.99		52.02	0.55				100.17	
	amphibole	47.87	0.47	10.13		3.11	0.16	17.99	0.26	11.28	3.01		95.08	Os-Ir-Ru
	amphibole	48.18		12.85		2.74	0.12	17.58	0.32	11.28	1.51		94.58	
	amphibole	46.53		11.56		2.76	0.05	20.82	0.62	12.31	1.59		96.24	
	amphibole	49.42		5.74	0.34	3.44		19.45	0.46	12.96	2.97		94.78	
Placers of the Aunik River (3)	olivine	39.3				6.10	0.1	48.7	0.3				94.5	
	olivine	41.9				7.80	0.2	51.7	0.3				101.9	Os-Ir-Ru
	amphibole	48.10		10.10	0.40	8.60	0.20	35.20	1.10	10.30	2.00		97.80	
	amphibole	49.90		7.10	0.30	11.00		35.00	1.10	7.20	1.60	0.10	97.80	
Mayarí-Cristal ophiolitic massif (1)	olivine	41.37		0.02	0.47	4.01	0.06	53.85	1.00	0.01			100.79	
	amphibole	46.41	0.7	10.19	2.84	2.30	0.05	20.3		11.86	2.67	0.08	99.5	chromite
	amphibole	47.38	0.6	8.9	2.58	1.97	0.01	22.12		10.37	2.44	0.16	98.69	
	amphibole	44.63	0.5	11.7	2.95	2.23	0.07	19.61	0.18	12.21	2.76	0.07	99.05	
Alapaevsk ophiolitic massif (2)	olivine	42.92			0.47	3.10	0.01	53.97	0.34				100.81	
	amphibole	44.40	0.41	9.81	3.25	2.78	0.09	19.65	0.05	12.34	3.30	0.66	96.76	chromite
	amphibole	46.79	2.02	9.60	2.34	2.77	0.08	19.48	0.09	11.89	2.50	0.04	97.18	

Note: the data used (1)—[48], (2)—[49], (3)—[46].

The second type of inclusions is micrometric and drop-shaped inclusions of base-metal sulfides with a diameter of 10 μm found close to the edge in the Os-dominant alloy. There are two types of mineral phases based on their composition. The first is a monosulfide compound close to chalcocite $(Cu_{1.87}Fe_{0.11})_{\Sigma 1.98}S_{1.1}$ calculated for a total of 2 a.p.f.u., the second is a bornite-like compound of the composition $(Cu_{5.2}Fe_{0.71}Ni_{0.09})_{\Sigma 5.8}S_{4.2}$ (for 10 a.p.f.u.).

The third type is inclusions of PGE minerals. Simple sulfides and rarely sulfoarsenides form monomineralic inclusions (up to 25 μm), the compositions of which correlate with the composition of the host Os-Ir-Ru alloy. The inclusions contain: laurite, a nonstoichiometric phase $(Ru,Ir,Os)S_2$, irarsite, cherepanovite, and telluropalladinite (Table 3). Sulfo-arsenide, as well as seleno-telluride PGM compounds, either compose polyphase inclusions in the edge part of grains or form replacement rims, in some cases rather thick (up to 50 μm), which we describe below. Of particular interest is a large (100 μm) polymineralic inclusion in the Os-dominant alloy (Figure 6e). The bulk of the inclusion is represented by a thin mixture of sulfide and a small amount of arseno-selenide phases Os-Ir-Ru, in which there are several blebs of idiomorphic laurite and an intergrowth of gold with the Pd-Bi-Te phase. Gold is high-grade and microporous. The palladium phase is represented by a bismuth-containing analog of telluropalladinite—$Pd_{8.9}(Te_{2.7}Bi_{1.4})_{\Sigma 4.1}$ (for 13 a.p.f.u.). Along the inclusion boundary, we observe a micrometric rim without ruthenium-bearing Os-Ir alloy.

4.3. Rim on Os-Ir-Ru Alloys

More than half of the PGM grains have a rim. According to the conditions of their formation, based on the nature of the relationship between a rim and a primary matrix mineral, we attribute the rims to replacement. The replacement rims usually have heterogeneous, spotty microtextures, and do not have a sharp interface between the rim and the matrix material. According to the mineral composition and microtextural features, two types of rim can be distinguished. The first type is sulfo-arsenide rims (Figure 7). In some cases, these are thin, rhythmically banded, 20–50 μm edges along the grain edge. In other cases, they are thicker (up to 200 μm) and in some cases completely "encircle" the original grain. According to the mineral composition, zoning is usually traced in them from the central part to the outer edge of the grain. Sulfides (laurite, erlichmanite) are replaced by PGE sulfoarsenides (ruarsite, irarsite, hollingworthite), which make up the bulk (90%) of the rim, and then arsenides (iridarsenite, sperrylite).

Table 3. Compositions of inclusions PGM in grains of Ru-Os-Ir alloy minerals from the placer of the Kitoy River.

	Ru	Os	Ir	Rh	Pt	Pd	Ni	As	S	Te	Bi	Total
Laurite	52.25	6.87	2.29	1.71	bdl	bdl	bdl	bdl	36.35	bdl	bdl	99.47
Laurite	53.87	3.29	2.32	bdl	bdl	bdl	bdl	bdl	36.31	bdl	bdl	95.79
$(Ru,Ir,Os)S_2$	36.15	12.14	17.03	bdl	bdl	bdl	0.24	bdl	30.78	bdl	bdl	96.34
$(Ru,Ir,Os)S_2$	39.95	6.54	17.87	bdl	bdl	bdl	bdl	bdl	32.13	bdl	bdl	96.49
$(Ru,Ir,Os)S_2$	42.97	5.62	17.01	bdl	bdl	bdl	bdl	bdl	33.15	bdl	bdl	98.75
Irarsite	8.08	27.41	23.45	bdl	bdl	bdl	1.15	26.64	10.65	bdl	bdl	97.38
Cherepanovite	bdl	bdl	bdl	55.91	bdl	bdl	4.23	39.86	bdl	bdl	bdl	100
Telluropalladinite	bdl	bdl	bdl	bdl	bdl	66	bdl	bdl	bdl	19.8	14.74	100.54
Atomic proportions (per a total of 100 at.%)												
	Ru	Os	Ir	Rh	Pt	Pd	Ni	As	S	Te	Bi	Total
Laurite	31.45	1.02	0.71	0	0	0	0	0	66.82	0	0	100
Laurite	29.32	2.13	0.7	0.98	0	0	0	0	66.87	0	0	100
$(Ru,Ir,Os)S_2$	24.26	4.33	6.01	0	0	0	0.28	0	65.12	0	0	100
$(Ru,Ir,Os)S_2$	25.92	2.26	6.1	0	0	0	0	0	65.72	0	0	100
$(Ru,Ir,Os)S_2$	26.96	1.87	5.61	0	0	0	0	0	65.56	0	0	100
Irarsite	7.59	13.68	11.59	0	0	0	1.86	33.75	31.53	0	0	100
Cherepanovite	0	0	0	46.1	0	0	8.62	45.28	0	0	0	100
Telluropalladinite	0	0	0	0	72.32	0	0	0	0	19.34	8.34	100

Note. Results of EDS analysis are listed in weight%; "bdl" indicates that amounts of elements are below detection limits.
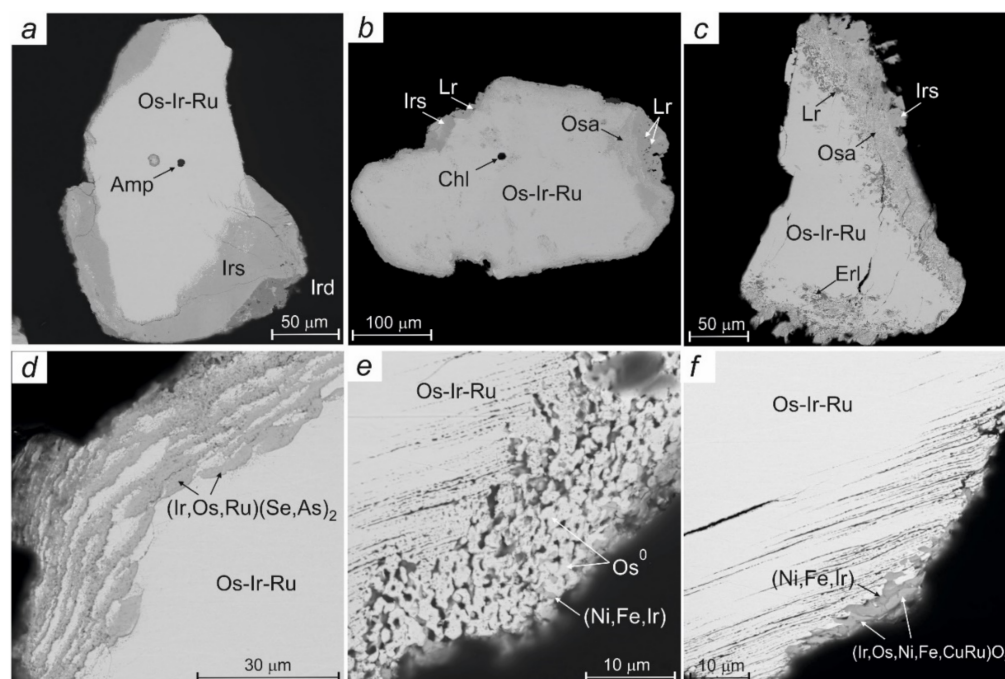

Figure 7. BSE images showing the rim around the grains of Os-Ir-Ru alloys, first type of rim: (**a**) wide rim of replacing Irarsite (Irs) and Iridarsenite (Ird); (**b**) complex rim of osarsite (Osa) and Irarsite (Irs) with laurite (Lr) inclusions; (**c**) rim sequentially folded from ehrlichmanite (Erl) and laurite (Lr), osarsite (Osa) and irarsite (Irs); second type of rim: (**d**) rhythmic-zonal rim of arseno-selenide; (**e**) micrometric grains of native osmium in a garutiite rim; (**f**) PGE oxide in intergrowth with garutiite in a thin rim.

The second type occurs in two grains of Os-dominant alloy with increased Ir content ($Os_{46.6}Ir_{35.1}Ru_{15.5}Fe_{1.3}Rh_{1.1}$; $Os_{42.7}Ir_{39.2}Ru_{17.6}Rh_{0.5}$). It is represented by rims and zones of alteration in a grain, developed by microcracks, and is composed of garutiite (Ni,Fe,Ir) [17,50,51] and micrometric (1–3 μm) rounded grains of newly formed phases of Os^0 and Os-Ir alloy (Table 4). A similar composition of garutiite was described in the works of J.A. Proenza et al. [52] and A.M. McDonald et al. [18] in the rims of Os-Ir-Ru alloys from the heavy fraction of chromitites from Loma Peguera (Dominican Republic). Garutiite is

in association with hexaferrum, ferruginous chromite, minerals of the chlorite group and serpentinite, awaruite, and irarsite.

Table 4. Compositions of the second type of rim of PGM in grains of Ru-Os-Ir alloy minerals from the placer of the Kitoy River.

	O	Fe	Co	Ni	Cu	Ru	Rh	Os	Ir	Total
Garutiite (Ni,Fe,Ir), wt.%										
garutiite	bdl	9.58	bdl	42.57	bdl	0.67	0	2.89	40.84	96.54
garutiite	bdl	36.58	1.16	15.73	bdl	1.34	0.37	bdl	43.9	99.07
garutiite	bdl	9.58	bdl	42.57	bdl	0.67	0	2.89	40.84	96.54
Neoformation phases—Os^0 and Os-Ir alloy, wt.%										
Os-Ir alloy	bdl	0.44	bdl	1.16	bdl	4.57	0	74.39	19.2	99.76
Os-Ir alloy	bdl	0.5	bdl	1.35	bdl	4.6	0	80.05	10.93	97.43
Os^0	bdl	0.41	bdl	0.78	bdl	2.51	0	85	12.64	101.33
Atomic proportions (per a total of 100 at.%)										
	O	Fe	Co	Ni	Cu	Ru	Rh	Os	Ir	Ni + Fe/∑PGE
garutiite	0	15.17	0	64.12	0	0.59	0	1.34	18.79	3.83
garutiite	0	55.14	1.66	22.56	0	1.12	0.3	0	19.23	3.76
garutiite	0	15.17	0	64.12	0	0.59	0	1.34	18.79	3.83
Os-Ir alloy	0	1.39	0	3.50	0	8.02	0	69.37	17.72	0
Os-Ir alloy	0	1.41	0	4.14	0	7.20	2.20	74.82	10.24	0
Os^0	0	1.31	0	2.38	0	4.45	0	80.08	11.78	0
PGE-Fe oxide phases, wt.%										
(Ir,Os,Ni,Fe,Cu,Ru)O$_2$	15.67	2.05	bdl	3.79	1.92	1.34	bdl	19.08	48.74	92.59
	O=1.98	**Atoms per formula unit (per a total of 3 apfu)**								∑ Ir,Os,Ni,Fe,Cu,Ru
(Ir,Os,Ni,Fe,Cu,Ru)O$_2$	1.98	0.07	0	0.13	0.06	0.03	0	0.20	0.52	1.02

Note. Results of EDS analysis are listed in weight%; "bdl" indicates that amounts of elements are below detection limits.

Between the newly formed micrometric phases, we found an oxide phase of PGE with a predominance of Ru and Ir. The size of the oxide does not allow the calculation of the mineral formula, but according to the atomic ratio, it corresponds to the AO$_2$ stoichiometry. Oxides of the PGE are currently described in the platinum mineralization of ophiolite complexes of the Urals, Finland, and Oman [9,17,53], including in the alluvial deposits of Chukotka [53,54], Gornaya Shoria [55], Western Sayan [23], among others.

4.4. PGE Selenides, Arsenoselenides, Tellurides

One of the features of PGM from alluvial deposits of the Kitoy River is the unusually wide development of alteration zones of Os-Ir-Ru alloys. The late mineral assemblage consists of selenium- and tellurium-containing mineral phases, which are unusual phases for PGE mineralization from ophiolite complexes. They form thin intermittent borders, inclusions in the marginal part of the grains, develop along grain cracks (Figure 8), weakened permeable zones, and in some cases almost completely replace the grain. They differ in variations in chemical composition. Three groups of compounds can be distinguished, which, according to the atomic ratio, correspond to the AB$_2$ stoichiometry. The most common group is the Os-Ir-Ru selenides, the second is the seleno-arsenides of Ir-Ru, Ir-Os-Ru, and Ru-Ir, and the third group is the tellurides of Os-Ir-Ru and Ru-Ir. Their formulas are shown in Table 5. The cationic portion of the compounds correlates generally with the composition of the host mineral.
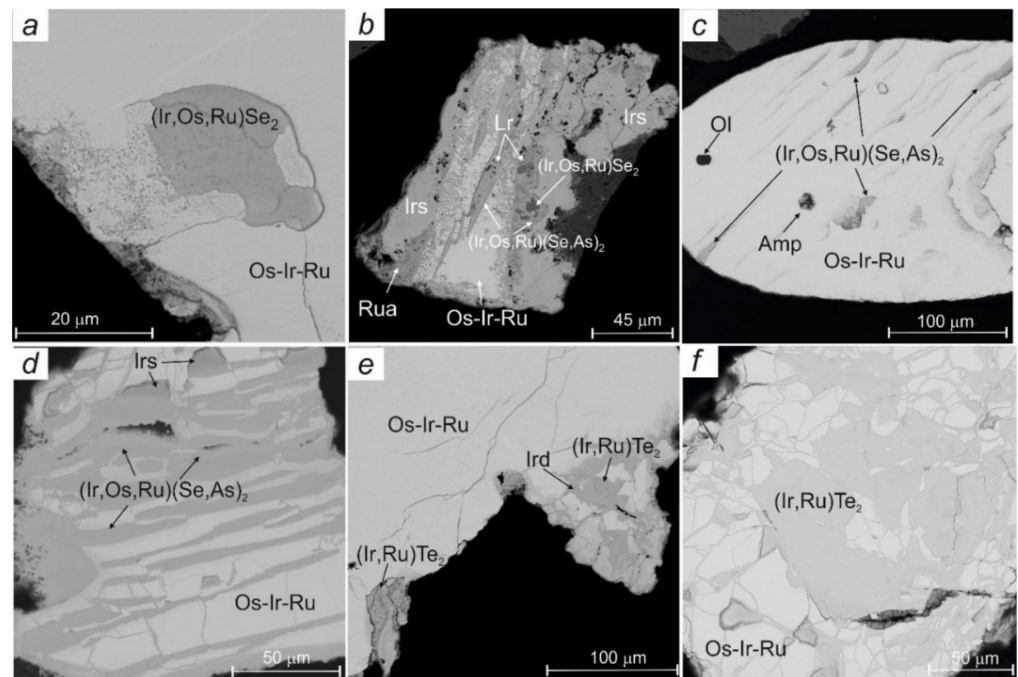
Figure 8. BSE images showing the development of alteration of secondary chalcogenides in Os-Ir-Ru alloys grains: (**a**) inclusion of IPGE selenide near the edge part; (**b**) grain is almost entirely replaced by laurite (Lr), irarsite (Irs), ruarsite, and selenium-containing compounds; (**c**) development of IPGE selenium-arsenides along microcracks in grain with inclusions of olivine and amphibole; (**d**) intensive development of irarsite (Irs), IPGE seleno-arsenides along microcracks in grain; (**e**) substitution of iridarsenite (Ird) by Ir-Ru telluride in the marginal part; (**f**) almost complete replacement of brecciated grain by Ir-Ru telluride.

Compounds of selenides and tellurides of the iridium subgroup of PGE (IPGE: Ir, Os, and Ru), as well as Se-rich phases of PGE, are exotic for ophiolite complexes. However, recently in the literature, there have been more and more references to findings of Se-enriched PGE compounds in ophiolite complexes and primitive ultrabasic rocks [22,23,46,56,57]. Barkov et al. [23] noted the predominance of stoichiometry of the AB_2 type for such compounds, with the formation of structures most optimal for the placement of Se under the given crystallization conditions. Earlier, we also described IPGE selenides with laurite-like structures in alluvial deposits of the r. Aunik (Western Transbaikalia) and in chromitites of the Dunzhugur ophiolite massif (Eastern Sayan) [46,57]. In the River Kitoy placer, we see a wide variety of similar compounds with a ratio of 1:2. Research into the synthetic platinum-group chalcogenides shows that osmium and ruthenium crystallize as compounds exclusively with the cubic structure of pyrite. Rhodium and iridium form a variety of chalcogenides differing in stoichiometry and structural patterns [58]. The structure of iridium selenide corresponds to the structure of marcasite and crystallizes in an orthorhombic crystal system [59], which is probably true for arsenoselenides upon replacement of As by selenium.

Table 5. Compositions of tellurides, selenides, and arsenosulfoselenides PGM in grains of Ru-Os-Ir alloy minerals from the placer of the Kitoy River.

	S	Ni	As	Se	Ru	Rh	Te	Os	Ir	Pt	Total
					Selenides						
$(Os,Ir,Ru)Se_2$	bdl	0.38	4.05	40.65	9.65	bdl	2.76	21.72	20.32	bdl	99.53
$(Os,Ir,Ru)Se$	bdl	bdl	3.36	44.12	10.47	bdl	2.83	24.39	19.35	bdl	104.52
$(Os,Ir,Ru)Se$	bdl	bdl	3,9	41.81	10.43	bdl	2.33	26.03	20.53	bdl	105.03
					Arsenoselenides						
$(Ir,Os,Ru,Rh)(Se,As)$	1.34	bdl	15.1	19.65	7.96	0.53	2.74	18.46	38.74	bdl	104.52
$(Ir,Ru,Pt,Rh,Os)(Se,As)$	0.8	bdl	13.97	33.54	16.74	0.6	1.07	1.87	24.66	6.46	99.72
$(Ir,Ru,Pt,Rh,Os)(Se,As)$	0.74	0.37	12.81	34.69	16.46	0.74	1.42	1.32	25.53	4.89	98.98
					Tellurides						
$(Ru,Ir)Te_2$	bdl	bdl	0.83	0.54	22.94	bdl	66.53	0	7.61	bdl	98.44
$(Ir,Ru)Te_2$	bdl	bdl	2.1	4.24	10.16	bdl	53.31	17.39	11.56	bdl	98.76
$(Ir,Ru)Te_2$	bdl	0.2	1.89	4.12	10.74	bdl	52.9	17.39	12.69	bdl	99.94
$(Ru,Ir)Te_2$	bdl	bdl	3.25	7.07	23.25	bdl	56.45	2.46	12.2	bdl	99.94
				Atomic proportions (per a total of 100 at%)							
	S	Ni	As	Se	Ru	Rh	Te	Os	Ir	Pt	Total
					Selenides						
$(Os,Ir,Ru)Se$	0	0.71	5.92	56.43	10.46	0	2.37	12.52	11.59	0	100
$(Os,Ir,Ru)Se$	0	0	4.68	58.31	10.81	0	2.31	13.38	10.51	0	100
$(Os,Ir,Ru)Se$	0	0	5.5	55.93	10.9	0	1.93	14.46	11.28	0	100
					Arsenoselenide						
$(Ir,Os,Ru,Rh)(Se,As)$	4.66	0	22.49	27.77	8.79	0.57	2.4	10.83	22.49	0	100
$(Ir,Ru,Pt,Rh,Os)(Se,As)$	2.53	0	18.89	43.02	16.77	0.59	0.85	1	13	3.35	100
$(Ir,Ru,Pt,Rh,Os)(Se,As)$	2.34	0.64	17.35	44.57	16.52	0.73	1.13	0.7	13.48	2.54	100
					Tellurides						
$(Ru,Ir)Te_2$	0	0	1.37	0.85	28.16	0	64.7	0	4.91	0	100
$(Ir,Ru)Te_2$	0	0	3.73	7.14	13.37	0	55.59	12.16	8	0	100
$(Ir,Ru)Te_2$	0	0.45	3.32	6.87	14	0	54.61	12.04	8.7	0	100
$(Ru,Ir)Te_2$	0	0	4.92	10.15	26.09	0	50.17	1.47	7.2	0	100
					Formula						
ASe_2	$(Os_{0.37}Ir_{0.35}Ru_{0.31}Ni_{0.02})_{\Sigma1.06}(Se_{1.69}As_{0.18}Te_{0.07})_{\Sigma1.94}$ $(Os_{0.4}Ir_{0.32}Ru_{0.32})_{\Sigma1.04}(Se_{1.75}As_{0.14}Te_{0.07})_{\Sigma1.96}$ $(Os_{0.43}Ir_{0.34}Ru_{0.33})_{\Sigma1.09}(Se_{1.68}As_{0.16}Te_{0.06})_{\Sigma1.9}$										
$A(Se,As)_2$	$(Ir_{0.67}Os_{0.32}Ru_{0.26}Rh_{0.02})_{\Sigma1.28}(Se_{0.83}As_{0.67}S_{0.14}Te_{0.07})_{\Sigma1.72}$ $(Ir_{0.39}Ru_{0.5}Os_{0.03}Rh_{0.02})_{\Sigma1.04}(Se_{1.29}As_{0.56}S_{0.08}Te_{0.03})_{\Sigma1.96}$ $(Ir_{0.4}Ru_{0.5}Pt_{0.08}Os_{0.02}Rh_{0.02}Ni_{0.02})_{\Sigma1.04}(Se_{1.33}As_{0.52}S_{0.07}Te_{0.03})_{\Sigma1.96}$										
ATe_2	$(Ru_{0.84}Ir_{0.15})_{\Sigma0.99}(Te_{1.94}As_{0.04}S_{0.02})_{\Sigma2.01}$ $(Os_{0.6}Ru_{0.4}Ir_{0.24})_{\Sigma1.01}(Te_{1.67}As_{0.21}S_{0.11})_{\Sigma1.99}$ $(Os_{0.6}Ru_{0.4}Ir_{0.24})_{\Sigma1.05}(Te_{1.64}As_{0.1}S_{0.05})_{\Sigma1.94}$ $(Ru_{0.78}Ir_{0.06}Os_{0.05})_{\Sigma1.04}(Te_{1.5}S_{0.3}As_{0.1})_{\Sigma1.96}$										

Note. Results of EDS analysis are listed in weight%; "bdl" indicates that amounts of elements are below detection limits.

5. Discussion

The presence of faceted PGM grains with crystal faces, their intergrowths, and a low degree of abrasion of most of the grains in the placer indicate their insignificant transfer from primary sources. The distances of transport thus were probably not great. The data based on the regional geology of the placer zones are also consistent with the inferred ophiolite sources. Indeed, outcrops of ophiolite complexes of the southern branch are exposed in the upper reaches of the Kitoy River and drained by its northern tributaries. The ophiolite source of PGM mineralization is also indicated by the ruthenium enrichment of primary melts and, accordingly, the accumulation of Ru during the crystallization of PGM alloys, reflected in the formation of the ruthenium trend (see Figure 2) [16,60–62].

In previous studies of ophiolite complexes of SEPES, we revealed differences in PGM mineralization of chromites taken from southern and northern ophiolite branches [28,41]. For chromitites of the northern branch, we noted the joint occurrence of Os-Ir-Ru compounds and Pt-bearing PGE minerals. In addition, here we observe a wide variety of low-temperature secondary PGMs: Pt-Cu, Pt-Pd-Cu, Pd-Hg, Rh_2SnCu, RhNiAs, $PtAs_2$, $PtSb_2$, and a wide development of PGE remobilization processes [28,29]. Above, we indicated (see Figure 1) a close relationship between the alluvial deposits of the Kitoy River and the ophiolite complexes of the southern (Ilchir) branch. The chromitites of the southern

ophiolite branch, and in particular the southern plate of the Ospa-Kitoy ophiolite complex, are dominated by Os-Ir-Ru solid solutions with a small amount of their sulfides and sulfoarsenides. In the alluvial placer along the Kitoy River, we also found only Os-Ir-Ru alloys. All of the above indicates that the main contribution to the placer was made by the chromitites of the ophiolites of the Southern branch of SEPES.

Silicate primary inclusions in PGMs, which we discovered and described, show a high degree of Mg-enrichment. We noted coexistence of high-Mg olivine (Fo90) and magnesian amphiboles inclusions, which are also highly magnesian (Mg# > 80). The increased contents of Al and Na in magnesio-hornblende from melt inclusions indicate high crystallization temperatures. We analyzed the composition of amphiboles and performed a calculated pressure assessment using amphibole geobarometers (Table 6, Figure 9). There are two groups of amphiboles: 1—magnesian hornblende (P = 7.5 kbar); 2—hornblende (magnesian-alkaline-ferruginous) (P = 3.5–4 kbar). This indicates the crystallization of amphiboles under different P-T conditions in a fluid-saturated environment. Features of the chemical composition of silicate inclusions indicate their formation from a magma and their relationship with primitive ultrabasic rocks. Thus, we believe that the grains of Os-Ir-Ru alloys crystallized at the magmatic stage under the conditions of the deep crust or uppermost mantle. This is confirmed by the peculiarities of the chemical composition of Os-Ir-Ru alloys with a magmatic ratio Os:Ir:Ru [47,63], the presence of laurite inclusions, and the presence of amphibole inclusions formed at a moderate pressure, which are formed under high-temperature conditions, in a reducing environment, during fluid-saturated environment.

Table 6. Amphiboles from inclusions in PGM grains, with P estimates (kbar).

Amphiboles	(1)	(2)	(3)	(4)	(5)
magnesio-hornblende	4	5	4.8	3.7	5
alumino-magnesio-hornblende	>7	7.9	8.1	6.2	7.9
tremolite	-	-	-	-	-
magnesio-hornblende	4	4.5	4.1	3.2	4.5
magnesio-hornblende	3	4	3.5	2.7	4
alumino-magnesio-hornblende	7	7.9	8.3	7.6	7.8

Note. Geobarometers: 1—[65], 2—[66]; 3—[67], 4—[68], 5—[69]. Pressure estimates are based on the empirical and experimental calibrations using aluminum content of hornblende. No data are provided where calculations of pressure are not impossible.
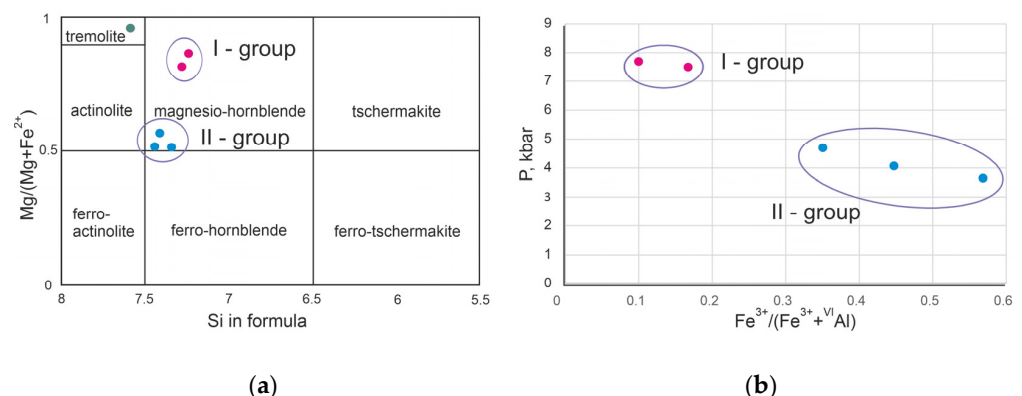

(**a**)   (**b**)

Figure 9. (**a**) Classification diagram of amphiboles [64], (**b**) a plot of $Fe^{3+}/(Fe^{3+} + {}^{VI}Al)$ vs. P, kbar for amphiboles from melt and crystalline inclusions in PGM.

As Os-Ir-Ru alloys crystallized, the residual melt (system) was enriched in ruthenium and PPGE. Ruthenium was actively included in the composition of Os-Ir-Ru alloys, forming a ruthenium trend in the triangular diagram. The increase in the content of rhodium impurities in later alloys (Ru-dominant Os-Ir-Ru alloys) is also related to this trend. As

the melt cooled, the amount of Pt and Fe increased until saturation of the system, with the formation of Pt-Fe alloy inclusions. Crystallization of sulfide and sulfoarsenide phases, with the formation of microinclusions, usually at the edge part of the grains, occurred with a decrease in temperature and against the background of an increase in fugacity of S_2 and As_2. During the crystallization of Os-Ir-Ru alloys in the restite melt, the content of minor components—base-metals Cu, Ni, Co, Fe—increased, and S, As, Se, Te, Sn, Bi, and Au accumulated in the residual fluid. The polyphase inclusion described above is a clear example of the capture of such a residual fluid with its further crystallization (see Figure 6f). We assume that sulfide high-temperature phases—idiomorphic laurite crystals—were the first to form from the residual melt. Sulfoarsenides and arsenides, irarsite, ruarsite, and gold formed from a complex eutectic (gold-silver-PGM sulfoarsenides) when the residual fluid phase further cooled. Palladium in the residual melt bonded with tellurium to form telluropalladinite.

Under post-magmatic conditions, autometasomatic transformations took place under the influence of a fluid phase, with the formation of a replacement rim. The zoning observed by us in the rims (from sulfides through sulfoarsenides to PGE arsenides) reflects the high fugacity of sulfur and arsenic in the fluid. As it cooled down, there was a gradual decrease in the activity of sulfur and an increase in the activity of arsenic in the system. The widespread development of tellurium- and selenium-containing phases is a consequence of the accumulation of Se and Te during progressive crystallization in a closed system. The initial high S/Se ratio in the mantle 2850–4350 [70,71] changed during the late evolutionary stage of the system under the influence of hydrothermal fluid. Sulfur is highly mobile in hydrothermal solutions, and in a fluid-saturated medium associated with zones of metasomatic alteration, it is likely to leave the system. This causes an increase in the fugacity of Se and the formation of various selenium-containing compounds with a critical decrease in the S/Se value. Taking into account the ability of Se to easily replace S in compounds, we can assume that the removal of S causes the incorporation of selenium into already existing compounds with the formation of selenides and arsenoselenides.

The discovery of complex rims of transformation of the garutiite composition with native osmium and PGE oxides, their morphology, and their structure allow us to interpret them as rims formed at low temperatures during post-magmatic processes, such as serpentinization/lateritization under the influence of metamorphic fluids [51,72,73]. Intensive changes in PGMs occur under the fluid-rock interaction with the participation of reduced gases (H_2, CH_4) and H_2O, desulfurization, and dearsenitization processes take place. Under conditions of temperature changes, Eh-pH changes in the Os-S-O-H system, low $f(S_2)$ and exposure to an oxidizing high-temperature fluid at a temperature of about 500 °C [74], Os becomes more mobile than other PGE, which leads to further redistribution and re-precipitation of osmium. The processes of remobilization of primary PGE and the formation of secondary minerals in the studied PGM grains are represented by native osmium, Os-Ir alloy, (Ni,Fe,Ir) [28,41]. The newly formed products are nano-sized particles, small crystallites, or rarely micrometric grains primarily sited on substrates of precursor detrital PGM grains. In the weathering zone, PGE sulfides and arsenides are destroyed under the action of oxidation in an aqueous medium and PGE oxides—hydroxides occur more or less in situ [75]. The formation of a PGE oxide, $(Ir,Os,Ni,Fe,CuRu)O_2$, which we found in the rim, is associated with the same processes. We believe that PGE oxides are formed during low-temperature replacement of rocks [9] or even grains in a diagenetic process or low-temperature metamorphism [52,53,76]. Their presence indicates the existence of mechanisms of PGE transport (in the form of oxide-hydroxide) under surface conditions, which facilitate the redistribution and crystallization of PGE during laterite weathering [77] or during serpentinization [78].

6. Conclusions

The source of platinum group minerals from the alluvial placer of the Kitoy River is the rocks of the Southern (Ilchir) ophiolite branch of SEPES and, in particular, the southern plate of the Ospa-Kitoy ophiolite complex, and primarily chromitites.

Platinum-group minerals were formed in several stages:

- Magmatic stage. At this stage high-temperature Os-Ir-Ru alloys with the magmatic ratio Os:Ir:Ru and homogeneous grain microstructure are formed under conditions of the deep crust or uppermost mantle;

- Late magmatic stage. With magmatic system cooling, volatile components, such as S and As, accumulate with the formation of the residual fluid phase. The residual fluid phase interacts with early platinum group minerals. High-temperature Os-Ir-Ru alloys are replaced by PGE sulfides and sulfoarsenides in the Os-Ir-Ru-Pt system.

- Postmagmatic stage. This stage is associated with the widespread development of arseno-selenides, selenides and tellurides of PGE. We assume that in the process of obduction of ophiolite complexes, the reducing conditions changed to oxidizing ones. The formation of selenides, PGE arsenides could be associated with a low S/Se ratio, due to the effective removal of S, which is more mobile than Se, in a fluid-saturated environment. These processes can also occur at the subduction stage, in which case the selenides will replace the previously formed sulfides and sulfoarsenides of PGE. The crushed grains filled with arsenoselenides and tellurides of PGE were probably formed at the stage of obduction of ophiolites and tectonic deformations. At the stage of obduction and orogeny, gold deposits were formed on the territory of the Eastern Sayan, in which telluride mineralization was established.

- Metamorphic stage. At stage of remobilization and re-deposition of PGE under metamorphic conditions native osmium, Os-Ir alloy and garutiite (Ni,Fe,Ir) were formed. Secondary PGM (e.g., native Os, intermetallic compounds of Ni, Fe and PGE) form or were modified at relatively low temperature during some post magmatic stage, possibly serpentinization or weathering.

Author Contributions: Conceptualization, E.V.A. and O.N.K.; methodology, D.K.B. and O.N.K.; software, D.K.B.; validation, S.M.Z., E.V.A. and O.N.K.; investigation, O.N.K. and E.V.A.; resources. Y.C.O.; data curation, S.M.Z., E.V.A. and O.N.K.; writing—original draft preparation, E.V.A.; writing—review and editing, E.V.A., O.N.K. and D.K.B.; visualization, E.V.A. and D.K.B.; supervision, E.V.A.; project administration, E.V.A.; funding acquisition, O.N.K. All authors have read and agreed to the published version of the manuscript.

Data Availability Statement: The data presented in this study are available in the article.

Conflicts of Interest: The authors declare no conflict of interest.

References

1. Maurel, C.; Maurel, P. Étude expérimentale de la distribution de l'aluminium entre bain silicaté basique et spinelle chromifère. Implications pétrogénétiques: Teneur en chrome des spinelles. *Bull. Minéralogie* **1982**, *105*, 197–202. [CrossRef]
2. Barnes, S.J.; Naldrett, A.J.; Gorton, M.P. The origin of the fractionation of platinum-group elements in terrestrial magmas. *Chem. Geol.* **1985**, *53*, 303–323. [CrossRef]
3. Rollinson, H. The geochemistry of mantle chromitites from the northern part of the Oman ophiolite: Inferred parental melt compositions. *Contrib. Mineral. Petrol.* **2008**, *156*, 273–288. [CrossRef]
4. Prichard, H.M.; Economou-Eliopoulos, M.; Fisher, P.C. Contrasting platinum-group mineral assemblages from two different podiform chromitite localities in the Pindos ophiolite complex, Greece. *Can. Mineral.* **2008**, *46*, 329–341. [CrossRef]

5. González-Jiménez, J.M.; Augé, T.; Gervilla, F.; Bailly, L.; Proenza, J.A.; Griffin, W.L. Mineralogy and geochemistry of platinum-rich chromitites from the mantle-crust transition zone at Ouen Island, New Caledonia Ophiolite. *Can. Mineral.* **2011**, *49*, 1549–1569. [CrossRef]

6. Ahmed, A.H. Highly depleted harzburgite–dunite–chromitite complexes from the Neoproterozoic ophiolite, south Eastern Desert, Egypt: A possible recycled upper mantle lithosphere. *Precambrian Res.* **2013**, *233*, 173–192. [CrossRef]

7. Melcher, F.; Grum, W.; Simon, G.; Thalhammer, T.V.; Stumpfl, E.F. Petrogenesis of the Ophiolitic Giant Chromite Deposits of Kempirsai, Kazakhstan: A Study of Solid and Fluid Inclusions in Chromite. *J. Petrol.* **1997**, *38*, 1419–1458. [CrossRef]

8. Nakagawa, M.; Franco, H.E.A. Placer Os-Ir-Ru alloys and sulfides: Indicators of sulfur fugacity in an ophiolite? *Can. Mineral.* **1997**, *35*, 1441–1452.

9. Ballhaus, C. Origin of podiform chromite deposits by magma mingling. *Earth Planet. Sci. Lett.* **1998**, *156*, 185–193. [CrossRef]

10. Zhou, M.F.; Sun, M.; Keays, R.R.; Kerrich, R.W. Controls on Platinum-Group Elemental Distributions of Podiform Chromitites: A Case Study of High-Cr and High-Al Chromitites from Chinese Orogenic Belts. *Geochim. Cosmochim. Acta* **1998**, *62*, 677–688. [CrossRef]

11. Barnes, S.J.; Roeder, P.L. The Range of Spinel Compositions in Terrestrial Mafic and Ultramafic Rocks. *J. Petrol.* **2001**, *42*, 2279–2302. [CrossRef]

12. Andrews, D.R.A.; Brenan, J.M. Phase equilibrium constraints on the magmatic origin of laurite+Ru-Os-Ir alloy. *Can. Mineral.* **2002**, *40*, 1705–1716. [CrossRef]

13. Ahmed, A.H.; Arai, S. Platinum-group minerals in podiform chromitites of the Oman ophiolite. *Can. Mineral.* **2003**, *41*, 597–616. [CrossRef]

14. Garuti, G. Chromite-platinum-group element magmatic deposits. In *Geology, Encyclopedia of Life Support Systems (EOLSS)*; de Vivo, B., Grasemann, B., Stüwe, K., Eds.; EOLSS Publisher: Oxford, UK, 2004.

15. Crocket, J.H. Platinum-group element geochemistry of mafic and ultramafic rocks. In *The Geology, Geochemistry, Mineralogy and Mineral Beneficiation of Platinum-Group Elements*; Cabri, L.J., Ed.; Canadian Institute of Mining Metallurgy and Petroleum: Montreal, QC, Canada, 2002; Volume 54, pp. 177–210, ISBN 9781894475273.

16. Bird, J.M.; Bassett, W.A. Evidence of a deep mantle history in terrestrial osmium-iridium-ruthenium alloys. *J. Geophys. Res. Solid Earth* **1980**, *85*, 5461–5470. [CrossRef]

17. Garuti, G.; Zaccarini, F. In situ alteration of platinum-group minerals at low temperature; evidence from serpentinized and weathered chromitite of the Vourinos Complex. *Can. Mineral.* **1997**, *35*, 611–626.

18. Mc Donald, A.M.; Proenza, J.A.; Zaccarini, F.; Rudashevsky, N.S.; Cabri, L.J.; Stanley, C.J.; Rudashevsky, V.N.; Melgarejo, J.C.; Lewis, J.F.; Longo, F.; et al. Garutiite, (Ni,Fe,Ir), a new hexagonal polymorph of native Ni from Loma Peguera, Dominican Republic. *Eur. J. Mineral.* **2010**, *22*, 293–304. [CrossRef]

19. González-Jiménez, J.M.; Reich, M.; Camprubí, A.; Gervilla, F.; Griffin, W.L.; Colás, V.; O'Reilly, S.Y.; Proenza, J.A.; Pearson, N.J.; Centeno-García, E. Thermal metamorphism of mantle chromites and the stability of noble-metal nanoparticles. *Contrib. Mineral. Petrol.* **2015**, *170*, 1–20. [CrossRef]

20. Agafonov, L.V.; Kuzhuget, K.S.; Oydup, C.K.; Stupakov, S.I. *Native Metals in Ultramafic Massifs of Tuva*; Velinskiy, V., Ed.; UIGGM: Novosibirsk, Russia, 1993; p. 86, ISBN 5762307336. (In Russian)

21. Podlipsky, M.Y.; Krivenko, A.P.; Polyakov, G.V. Platinum-palladium mineralization in chromite ores from ultrabasic rocks of the western Sayan region. *Dokl. Earth Sci.* **2004**, *396*, 508–511.

22. Tolstykh, N.D.; Krivenko, A.P.; Pospelova, L.N. Unusual compounds of iridium, osmium and ruthenium with selenium, tellurium and arsenic from placers of the Zolotaya River (western Sayans). *Zap. Vsesoyuzn. Miner. Obs.* **1997**, *126*, 23–34. (In Russian)

23. Barkov, A.Y.; Shvedov, G.I.; Silyanov, S.A.; Martin, R.F. Mineralogy of Platinum-Group Elements and Gold in the Ophiolite-Related Placer of the River Bolshoy Khailyk, Western Sayans, Russia. *Minerals* **2018**, *8*, 247. [CrossRef]

24. Barkov, A.Y.; Tamura, N.; Shvedov, G.I.; Stan, C.V.; Ma, C.; Winkler, B.; Martin, R.F. Platiniferous Tetra-Auricupride: A Case Study from the Bolshoy Khailyk Placer Deposit, Western Sayans, Russia. *Minerals* **2019**, *9*, 160. [CrossRef]

25. Orsoev, D.A.; Tolstykh, N.D.; Kislov, E.V. PtCu$_3$ composition mineral from chromitites of Ospinsko-Kitoisky ultramafic massif (Eastern Sayans). *Zap. Vserossiyskogo Mineral. Obs.* **2001**, *130*, 61–70. (In Russian)

26. Zhmodik, S.M.; Mironov, A.G.; Agafonov, L.V.; Zhmodik, A.S.; Pavlov, A.L.; Moroz, T.N.; Airiyants, E.V.; Kulikov, Y.L.; Borovikov, A.A.; Ponomarchuk, V.A.; et al. Carbonization of east Sayan ultrabasic rocks and Au-Pd-Pt mineralization. *Russ. Geol. Geophys.* **2004**, *45*, 210–225.

27. Zhmodik, S.M.; Postnikov, A.A.; Buslov, M.M.; Mironov, A.G. Geodynamics of the Sayan-Baikal-Muya accretion-collision belt in the neoproterozoic-early paleozoic and regularities of the formation and localization of precious-metal mineralization. *Russ. Geol. Geophys.* **2006**, *47*, 187–201.

28. Kiseleva, O.N.; Zhmodik, S.M.; Damdinov, B.B.; Agafonov, L.V.; Belyanin, D.K. Composition and evolution of PGE mineralization in chromite ores from the Il'chir ophiolite complex (Ospa–Kitoi and Khara-Nur areas, East Sayan). *Russ. Geol. Geophys.* **2014**, *55*, 259–272. [CrossRef]

29. Kiseleva, O.; Zhmodik, S. PGE mineralization and melt composition of chromitites in Proterozoic ophiolite complexes of Eastern Sayan, Southern Siberia. *Geosci. Front.* **2017**, *8*, 721–731. [CrossRef]

30. Kiseleva, O.N. Chromitites and Platinum-Metal Mineralization in the Ophiolites of the Southeastern Part of the Eastern Sayan. Ph.D. Thesis, Institute of Geology and Mineralogy of the Siberian Branch of Russian Academy of Science IGM SB RAS, Novosibirsk, Russia, 2014. (In Russian)
31. Dobretsov, N.L.; Konnikov, E.G.; Dobretsov, N.N. Precambrian ophiolite belts of southern Siberia, Russia, and their metallogeny. *Precambrian Res.* **1992**, *58*, 427–446. [CrossRef]
32. Belichenko, V.G.; Butov, Y.P.; Boos, R.G.; Vratkovskaya, S.V.; Dobretsov, N.L.; Dolmatov, V.A.; Zhmodik, S.M.; Konnikov, E.G.; Kuzmin, M.I.; Medvedev, V.N.; et al. *Geology and Metamorphism of the East Sayan*; Nauka: Novosibirsk, Russia, 1988. (In Russian)
33. Gordienko, I.V.; Dobretsov, N.L.; Zhmodik, S.M.; Roshchektaev, P.A. Multistage Thrust and Nappe Tectonics in the Southeastern Part of East Sayan and Its Role in the Formation of Large Gold Deposits. *Russ. Geol. Geophys.* **2021**, *62*, 109–120. [CrossRef]
34. Kuzmichev, A.B.; Sklyarov, E.V.; Letnikova, E.F.; Gladkochub, D.F.; Khain, E.V. Neoproterozoic ophiolite and sedimentary sequences of the Tuva-Mongolian superterrane. In Proceedings of the Assembly and Breakup of Rodinia Supercontinent: Evidence from South Siberia; Guide-Book and Abstracts of the IGCP-440 Workshop. Sklyarov, E.V., Ed.; Publishing House of Institute of Earth Crust: Irkutsk, Russia, 2001; pp. 71–92. (In Russian)
35. Fedorovskii, V.S.; Khain, E.V.; Vladimirov, A.G.; Kargopolov, S.A.; Gibsher, A.S.; Izokh, A.E. Tectonics, metamorphism, and magmatism of collisional zones of the Central Asian Caledonides. *Geotectonics* **1995**, *29*, 193–212.
36. Dobretsov, N.L. About the cover tectonics of the Eastern Sayan [O pokrovnoy tektonike Vostochnogo Sayana]. *Geotektonika* **1985**, *1*, 39–50. (In Russian)
37. Sklyarov, E.V.; Kovach, V.P.; Kotov, A.B.; Kuzmichev, A.B.; Lavrenchuk, A.V.; Perelyaev, V.I.; Shchipansky, A.A. Boninites and ophiolites: Problems of their relations and petrogenesis of boninites. *Russ. Geol. Geophys.* **2016**, *57*, 127–140. [CrossRef]
38. Kuzmichev, A.B.; Larionov, A.N. Neoproterozoic island arcs in East Sayan: Duration of magmatism (from U–Pb zircon dating of volcanic clastics). *Russ. Geol. Geophys.* **2013**, *54*, 34–43. [CrossRef]
39. Zhmodik, S.; Kiseleva, O.; Belyanin, D.; Damdinov, B.; Airiyants, E.; Zhmodik, A. PGE mineralization in ophiolites of the southeast part of the Eastern Sayan (Russia). In Proceedings of the 12th International Platinum Symposium, Yekaterinburg, Russia, 11–14 August 2014; Russian Academy of Sciences; Zavaritsky Institute of Geology and Geochemistry (IGG UB RAS): Yekaterinburg, Russia, 2014; pp. 221–222.
40. Kiseleva, O.N.; Airiyants, E.V.; Belyanin, D.K.; Zhmodik, S.M.; Ashchepkov, I.V.; Kovalev, S.A. Multistage Magmatism in Ophiolites and Associated Metavolcanites of the Ulan-Sar'dag Mélange (East Sayan, Russia). *Minerals* **2020**, *10*, 1077. [CrossRef]
41. Kiseleva, O.N.; Airiyants, E.V.; Belyanin, D.K.; Zhmodik, S.M. Podiform Chromitites and PGE Mineralization in the Ulan-Sar'dag Ophiolite (East Sayan, Russia). *Minerals* **2020**, *10*, 141. [CrossRef]
42. Orsoev, D.A.; Ochirov, Y.C.; Mironov, A.G.; Damdinov, B.B.; Zhmodik, S.M. Platinum metal minerals and types of their associations in gold placers of the Sayan-Baikal folded area (Buryatia). *Russ. Geol. Geophys.* **2004**, *45*, 335–346.
43. Garuti, G.; Zaccarini, F.; Cabella, R.; Fershtater, G. Occurrence of unknown Ru-Os-Ir-Fe oxides in the chromitites of the Nurali ultramafic complex, Southern Urals, Russia. *Can. Mineral.* **1997**, *35*, 1431–1439.
44. Tolstykh, N.D.; Sidorov, E.; Laajoki, K.V.O.; Krivenko, A.P.; Podlipskiy, M. The association of platinum-group minerals in placers of the Pustaya River, Kamchatka, Russia. *Can. Mineral.* **2000**, *38*, 1251–1264. [CrossRef]
45. Zaykov, V.V.; Melekestseva, I.Y.; Zaykova, E.V.; Kotlyarov, V.A.; Kraynev, Y.D. Gold and platinum group minerals in placers of the South Urals: Composition, microinclusions of ore minerals and primary sources. *Ore Geol. Rev.* **2017**, *85*, 299–320. [CrossRef]
46. Airiyants, E.V.; Belyanin, D.K.; Zhmodik, S.M.; Agafonov, L.V.; Romashkin, P.A. Chemical composition and origin of platinum-group minerals from placers of the Aunik River, Buryatia, Russia. *Ore Geol. Rev.* **2020**, *120*, 103453. [CrossRef]
47. Cabri, L.J.; Harris, D.C.; Weiser, T.W. Mineralogy and distribution of platinum-group mineral (PGM) placer deposits of the world. *Explor. Min. Geol.* **1996**, *5*, 73–167.
48. González-Jiménez, J.M.; Proenza, J.A.; Gervilla, F.; Melgarejo, J.C.; Blanco-Moreno, J.A.; Ruiz-Sánchez, R.; Griffin, W.L. High-Cr and high-Al chromitites from the Sagua de Tánamo district, Mayarí-Cristal ophiolitic massif (eastern Cuba): Constraints on their origin from mineralogy and geochemistry of chromian spinel and platinum-group elements. *Lithos* **2011**, *125*, 101–121. [CrossRef]
49. Zaccarini, F.; Pushkarev, E.; Garuti, G.; Kazakov, I. Platinum-Group Minerals and Other Accessory Phases in Chromite Deposits of the Alapaevsk Ophiolite, Central Urals, Russia. *Minerals* **2016**, *6*, 108. [CrossRef]
50. Aiglsperger, T.; Proenza, J.A.; Font-Bardia, M.; Baurier-Aymat, S.; Galí, S.; Lewis, J.F.; Longo, F. Supergene neoformation of Pt-Ir-Fe-Ni alloys: Multistage grains explain nugget formation in Ni-laterites. *Miner. Depos.* **2016**, *52*, 1069–1083. [CrossRef]
51. Aiglsperger, T.; Proenza, J.A.; Zaccarini, F.; Lewis, J.F.; Garuti, G.; Labrador, M.; Longo, F. Platinum group minerals (PGM) in the Falcondo Ni-laterite deposit, Loma Caribe peridotite (Dominican Republic). *Miner. Depos.* **2014**, *50*, 105–123. [CrossRef]
52. Proenza, J.A.; Zaccarini, F.; Lewis, J.F.; Longo, F.; Garuti, G. Chromian spinel composition and the platinum group minerals of the PGE-rich Loma Peguera chromitites, Loma Caribe peridotite, Dominican Republic. *Can. Mineral.* **2007**, *45*, 631–648. [CrossRef]
53. Gornostayev, S.S.; Crocket, J.H.; Mochalov, A.G.; Laajoki, K.V.O. The platinum-group minerals of the Baimka placer deposits, Aluchin Horst, Russian Far East. *Can. Mineral.* **1999**, *37*, 1117–1129.
54. Mochalov, A.G.; Dmitrenko, G.G.; Khoroshilova, T.S.; Sakhyanov, L.O. Mineralogical and geochemical types of placers of platinoids and their industrial significance. In Proceedings of the Mineralogy and Geochemistry of Placers; Shilo, N.A., Patyk-Kara, N.G., Eds.; Nauka: Moscow, Russia, 1992; pp. 7–23. (In Russian)

55.	Zhmodik, S.M.; Nesterenko, G.V.; Airiyants, E.V.; Belyanin, D.K.; Kolpakov, V.V.; Podlipsky, M.Y.; Karmanov, N.S. Alluvial platinum-group minerals as indicators of primary PGE mineralization (placers of southern Siberia). *Russ. Geol. Geophys.* **2016**, *57*, 1437–1464. [CrossRef]

56.	Barkov, A.Y.; Nikiforov, A.A.; Tolstykh, N.D.; Shvedov, G.I.; Korolyuk, V.N. Compounds of Ru–Se–S, alloys of Os–Ir, framboidal Ru nanophases, and laurite–clinochlore intergrowths in the Pados-Tundra complex, Kola Peninsula, Russia. *Eur. J. Mineral.* **2017**, *29*, 613–621. [CrossRef]

57.	Kiseleva, O.; Airiyants, E.; Zhmodik, S.; Belyanin, D. Ruthenium selenides in chromitites Dunzhugur ophiolite complex. In Proceedings of the Problems of Geology and Exploitation of Platinum Metal Deposits; Talovina, I., Ed.; Saint Petersburg Mining University: Saint Petersburg, Russia, 2016; pp. 71–74. (In Russian)

58.	Dey, S.; Jain, V.K. Platinum group metal chalcogenides: Their syntheses and applications in catalysis and materials science. *Platin. Met. Rev.* **2004**, *48*, 16–29.

59.	Guo, J.; Qi, Y.; Matsuishi, S.; Hosono, H. T c maximum in solid solution of pyrite IrSe2- RhSe2 induced by destabilization of anion dimers. *J. Am. Chem. Soc.* **2012**, *134*, 20001–20004. [CrossRef]

60.	Tolstykh, N.D.; Sidorov, E.G.; Krivenko, A.P. Platinum-Group Element Placers Associated with Ural-Alaska Type Complexes. In *Mineralogical Association of Canada Short Course Series Volume 35*; Mungall, J.E., Ed.; The Mineralogical Association of Canada: Quebec City, QC, Canada, 2005; pp. 113–143, ISBN 0921294352.

61.	Tolstykh, N.; Krivenko, A.; Sidorov, E.; Laajoki, K.; Podlipsky, M. Ore mineralogy of PGM placers in Siberia and the Russian Far East. *Ore Geol. Rev.* **2002**, *20*, 1–25. [CrossRef]

62.	Weiser, T.W.; Bachmann, H.G. Platinum-group minerals from the Aikora River area, Papua New Guinea. *Can. Mineral.* **1999**, *37*, 1131–1145.

63.	O'Driscoll, B.; González-Jiménez, J.M. Petrogenesis of the Platinum-Group Minerals. *Rev. Mineral. Geochem.* **2016**, *81*, 489–578. [CrossRef]

64.	Leake, B.E.; Woolley, A.R.; Arps, C.E.S.; Birch, W.D.; Gilbert, M.C.; Grice, J.D.; Hawthorne, F.C.; Kato, A.; Kisch, H.J.; Krivovichev, V.G.; et al. Nomenclature of amphiboles; report of the subcommittee on amphiboles of the International Mineralogical Association, Commission on New Minerals and Mineral Names. *Can. Mineral.* **1997**, *35*, 219–246.

65.	Mishkin, M.A. Amphibole geobarometr for metabasites. *Dokl. AN SSSR* **1990**, *312*, 944–946. (In Russian)

66.	Hammarstrom, J.M.; Zen, E. Aluminum in hornblende: An empirical igneous geobarometer. *Am. Mineral.* **1986**, *71*, 1297–1313.

67.	Hollister, L.S.; Grissom, G.C.; Peters, E.K.; Stowell, H.H.; Sisson, V.B. Confirmation of the empirical correlation of Al in hornblende with pressure of solidification of calc-alkaline plutons. *Am. Mineral.* **1987**, *72*, 231–239.

68.	Johnson, M.C.; Rutherford, M.J. Experimental calibration of the aluminum-in-hornblende geobarometer with application to Long Valley caldera (California) volcanic rocks. *Geology* **1989**, *17*, 837–841. [CrossRef]

69.	Schmidt, M.W. Amphibole composition in tonalite as a function of pressure: An experimental calibration of the Al-in-hornblende barometer. *Contrib. Mineral. Petrol.* **1992**, *110*, 304–310. [CrossRef]

70.	Lorand, J.P.; Alard, O.; Luguet, A.; Keays, R.R. Sulfur and selenium systematics of the subcontinental lithospheric mantle: Inferences from the Massif Central xenolith suite (France). *Geochim. Cosmochim. Acta* **2003**, *67*, 4137–4151. [CrossRef]

71.	Smith, J.W.; Holwell, D.A.; McDonald, I.; Boyce, A.J. The application of S isotopes and S/Se ratios in determining ore-forming processes of magmatic Ni–Cu–PGE sulfide deposits: A cautionary case study from the northern Bushveld Complex. *Ore Geol. Rev.* **2016**, *73*, 148–174. [CrossRef]

72.	Bowles, J.F.W. The development of platinum-group minerals in laterites. *Econ. Geol.* **1986**, *81*, 1278–1285. [CrossRef]

73.	Bowles, J.F.W.; Lyon, I.C.; Saxton, J.M.; Vaughan, D.J. The Origin of Platinum Group Minerals from the Freetown Intrusion, Sierra Leone, Inferred from Osmium Isotope Systematics. *Econ. Geol.* **2000**, *95*, 539–548. [CrossRef]

74.	Xiong, Y.; Wood, S.A. Experimental quantification of hydrothermal solubility of platinum-group elements with special reference to porphyry copper environments. *Mineral. Petrol.* **2000**, *68*, 1–28. [CrossRef]

75.	Oberthür, T. The Fate of Platinum-Group Minerals in the Exogenic Environment—From Sulfide Ores via Oxidized Ores into Placers: Case Studies Bushveld Complex, South Africa, and Great Dyke, Zimbabwe. *Minerals* **2018**, *8*, 581. [CrossRef]

76.	Zaccarini, F.; Proenza, J.A.; Ortega-Gutiérrez, F.; Garuti, G. Platinum group minerals in ophiolitic chromitites from Tehuitzingo (Acatlán complex, southern Mexico): Implications for post-magmatic modification. *Mineral. Petrol.* **2005**, *84*, 147–168. [CrossRef]

77.	Bowles, J.F.W.; Suárez, S.; Prichard, H.M.; Fisher, P.C. The mineralogy, geochemistry and genesis of the alluvial platinum-group minerals of the Freetown Layered Complex, Sierra Leone. *Mineral. Mag.* **2018**, *82*, S223–S246. [CrossRef]

78.	Auge, T.; Legendre, O. Platinum-group element oxides from the Pirogues ophiolitic mineralization, New Caledonia; origin and significance. *Econ. Geol.* **1994**, *89*, 1454–1468. [CrossRef]